



Unveiling the molecular regulatory mechanisms of immune responses in the spleen of spotted sea bass (*Lateolabrax maculatus*) against *Nocardia seriolae* infection

Yani Dong^a, Haishen Wen^a, Yonghang Zhang^a, Xin Qi^a, Lingyu Wang^a, Hao Li^a, Kaiqiang Zhang^a, Yun Li^{a,b,*}

^a Key Laboratory of Mariculture, Ministry of Education (KLMME), Ocean University of China, Qingdao 266003, China

^b Sanya Oceanographic Institution, Ocean University of China, Qingdao, Shandong/Sanya, Hainan 266100/572025, China

ARTICLE INFO

Keywords:

Spotted sea bass
Nocardia seriolae
Bacterial infection
RNA-Seq
Alternative splicing

ABSTRACT

Spotted sea bass holds significant economic importance in China's aquaculture sector. The outbreaks of bacterial diseases, especially caused by *Nocardia seriolae* (*N. seriolae*), have occurred frequently due to intensive farming. With the high morbidity and mortality, fish nocardiosis is one of the most serious problems faced by the aquaculture industry of spotted sea bass. However, the regulatory mechanism of immune response in spotted sea bass after *N. seriolae* infection remain elusive. In our study, we conducted a comprehensive examination of clinical symptoms and histological structures of the spleen, revealing noticeable pathological changes in diseased fish. Subsequently, we employed transcriptome sequencing of the spleen to investigate the effect of *N. seriolae* on spotted sea bass at 0 h, 48 h, 96 h and 120 h at transcriptome level. A total of 3031, 3597, and 4683 differentially expressed genes (DEGs) were unveiled in 48 h vs. 0 h, 96 h vs. 0 h and 120 h vs. 0 h, respectively. Up-regulated DEGs were significantly enriched in PRRs and cytokine related pathways, while down-regulated DEGs exhibited significant enrichment in autophagy related pathways, suggesting potential roles in immune modulation. Weighted co-expression network analysis (WGCNA) identified a blue module strongly linked to the immune response against *N. seriolae* infection, from which 10 hub genes were identified, including *ilr2*, *tnfrsf9*, *c7* and so on. Moreover, our findings highlighted the involvement of alternative splicing (AS) in the immune response and found that pathogen infection also induced the AS events in some immune-related genes. Our study could shed new light on the molecular regulatory mechanisms underlying the immune response after *N. seriolae* infection in spotted sea bass, providing a basic guidance for the breeding of spotted sea bass with disease resistance in the future.

1. Introduction

The spotted sea bass (*Lateolabrax maculatus*) holds considerable economic importance in aquaculture with a wide distribution along the coast of China. The production of spotted sea bass has been increasing annually, reaching 218,053 tons in 2022, ranking third among marine aquaculture fish (China, 2023). However, alongside the development of aquaculture industry of spotted sea bass, degenerating water quality due to intensive farming and inadequate scientific breeding awareness of farmers, disease caused by various of bacteria or virus resulted in adverse impacts on production and huge economic losses.

Nocardia sp. is a gram-positive, aerobic and filamentous bacterium responsible for fish nocardiosis, characterized by its prolonged incubation period, high infection rates, and mortality. In recent years, various species of *Nocardia* have been isolated from infected fish and shellfish, including *Nocardia asteroides*, *Nocardia salmonicida*, *Nocardia crassostreae*, *Nocardia brasiliensis* and *Nocardia seriolae* (Acosta et al., 2024; Maekawa et al., 2018). Notably, *N. seriolae* has been documented to infect approximately 42 species of marine and freshwater teleost, and more commonly in sea perch (*Lateolabrax japonicus*), golden pompano (*Trachinotus ovatus*), northern snakehead (*Channa argus*), and large-mouth bass (*Micropterus Salmoides*) in China (Liu et al., 2023a). Infected

* Corresponding author.

E-mail addresses: dongyn0516@163.com (Y. Dong), wenhaishen@ouc.edu.cn (H. Wen), zyh220201@163.com (Y. Zhang), qx@ouc.edu.cn (X. Qi), wly4139@ouc.edu.cn (L. Wang), lihao2018@stu.ouc.edu.cn (H. Li), zkq@ouc.edu.cn (K. Zhang), yunli0116@ouc.edu.cn (Y. Li).

<https://doi.org/10.1016/j.aquaculture.2024.741178>

Received 10 April 2024; Received in revised form 29 May 2024; Accepted 5 June 2024

Available online 17 June 2024

0044-8486/© 2024 Elsevier B.V. All rights are reserved, including those for text and data mining, AI training, and similar technologies.

fish initially exhibit poor appetite in the early stage, followed by the accumulation of immune and epithelial cells around lesions, resulting in the formation of granuloma tissues, characterized by numerous white or grey nodules on gills and various organs, such as the spleen, kidney, liver and heart, accompanying congestion and bleeding on the body surface (Chen et al., 2000). The primary approach for preventing and controlling fish nocardiosis involves the administration of various antibiotics (Yasuike et al., 2017). However, the granuloma caused by *N. seriolae* infection will provide a physical barrier to hinder drug penetration and create a conducive environment for bacterial colonization, thereby compromising the efficacy of antibiotics treatments (Wang et al., 2017). Meanwhile, antibiotics usage will lead to serious concerns, like environmental contamination, food safety risks, and the emergence of drug-resistant *N. seriolae* strains, ultimately impact on human health (Kraemer et al., 2019). Hence, it is urgent for researchers to determine immune molecular mechanisms underlying defense against *N. seriolae* infection in spotted sea bass, with the aim of achieving efficient ecological breeding and disease prevention.

Innate immunity represents the primary host defense against invading pathogens, with fish relying predominantly on innate immune defenses compared to higher vertebrates (Buchmann, 2014). Pattern recognition receptors (PRRs), crucial for innate immunity, identify diverse pathogen-associated molecular patterns (PAMPs) (Li et al., 2020). PRRs can divide into membrane-bound toll-like receptors (TLRs) (Vijay, 2018), cytoplasmic NOD-like receptors (NLRs) (Kim et al., 2016), as well as other receptors, like RIG-I-like receptors (RLRs) and C-type lectin receptors (CLRs) (Xiu et al., 2016). Upon the activation of innate immunity, a cascade of downstream signaling molecules like cytokines and chemokines is produced (Kawai and Akira, 2010; Thaïss et al., 2016). Chemokines regulate immune cell migration and positioning during inflammation, serving as a crucial link between the innate and adaptive immunity (Sokol and Luster, 2015). Pathogen invasion will lead to host activated apoptosis and autophagy to maintain the cellular homeostasis. Apoptosis involved in the clearance of pathogen-infected cells to prevent the spread of harmful agents within the organism. Simultaneously, it could prevent excessive inflammation and tissue damage by eliminating activated immune cells after immune response. While autophagy facilitates the phagocytosis and degradation of compromised or senescent cells, making the cells more conducive to survival. Dysregulation of autophagy has been implicated in various immune-related disorders (Levine and Kroemer, 2019). The sophisticated interplay between apoptosis and autophagy is pivotal in determining cellular fate during immune responses (Maiuri et al., 2007).

In teleost, the molecular regulatory mechanisms of pathogens infection are far away from that in mammals. Leveraging advancements in next-generation sequencing technology, transcriptome profiling emerges as potent tool for dissecting immune-related genes expression profiles, thus unraveling host defense mechanisms against pathogenic onslaughts in teleost. In Yangtze sturgeon (*Acipenser dabryanus*), researchers have uncovered the immune response of Yangtze sturgeon after *Edwardsiella tarda* challenged (Chen et al., 2023). The relationship between neuroactive receptor genes and immunity has been identified in Nile tilapia (*Oreochromis niloticus*) after *Streptococcus agalactiae* infection (Hou et al., 2023). Bai et al. identified *cd82a* as a disease resistance gene in large yellow croaker after *Pseudomonas plecoglossicida* invasion (Bai et al., 2022). These studies demonstrate the utility of transcriptome analysis in elucidating the host immune response to bacterial infection in teleost, providing valuable insights into the molecular mechanisms underlying fish immunity. However, to our knowledge there have been no studies about transcriptome analysis for the identification of gene expression profiles in spotted sea bass against *N. seriolae* infection.

Therefore, in this investigation, 3 time points of infected spleens were chosen for sequencing to obtain time-dependent variations in the expression profiles of immune pathway related genes in spotted sea bass post *N. seriolae* infection. This transcriptome sequencing analysis aims to

pinpoint key genes engaged in regulating the immune response and elucidate hub gene regulation network of spotted sea bass infected with *N. seriolae*. Our findings offer basic directions for the breeding of spotted sea bass with disease-resistance in future.

2. Materials and methods

2.1. Animals and bacteria

Spotted sea bass (average weight: 53.22 ± 9.0 g, average length: 18.16 ± 1.2 cm) were obtained from Jinghai Marine Fisheries Co., Ltd. (Yantai, China). We randomly selected 10 fish to conduct morphological healthy examination and dissection to ensure their health conditions and absence of fish nocardiosis symptoms. The fish were acclimatized at 26°C for 2 weeks in a water circulation system and fed twice a day. The *N. seriolae* (WL-2021-1) was provided by Xia Liquan's research group of Shenzhen Institute of Guangdong Ocean University, which was initially isolated from snakehead with fish nocardiosis. The bacteria were cultivated in brain-heart infusion (BHI) broth at 28°C , followed by confirmation of their identity as *N. seriolae* through 16S-rDNA sequencing.

All fish experiments adhered to the guideline of the Animal Research and Ethics Committees of Ocean University of China (Permit Number: 20141201). No endangered or protected species were utilized in the experiment.

2.2. Bacterial challenge and sampling

N. seriolae were centrifuged at $5000 \times g$ for 15 min to separate the bacteria from culture medium. The bacterial pellet was then resuspended in $1 \times$ phosphate-buffered saline (PBS, pH 7.3) to adjust the bacterial concentration to 1×10^6 CFU/mL, as determined by preliminary experiments. Spotted sea bass were allocated into control and treatment groups, with three replicates per group, each containing 60 fish. Treatment groups were anesthetized and intraperitoneally injected with 100 μL suspension of 1×10^6 CFU/mL *N. seriolae*, while control group injected intraperitoneally with 100 μL PBS. Both the control and treatment groups were reared in separate tanks under the same conditions (temperature: $26.0 \pm 2.0^\circ\text{C}$) after injection.

The spleen tissues of treatment and control groups were dissected and sampled at 0 h, 48 h, 96 h and 120 h post-infection. Subsequently, they were promptly frozen in liquid nitrogen and stored at -80°C . Besides, spleen tissues were also sampled and fixed in 4% paraformaldehyde for 24 h to facilitate subsequent histological observations.

2.3. Morphological and histological analysis

The spleen tissues underwent dehydration using a series of ethanol (from 70% to 100%) after overnight tissue fixation. Subsequently, the samples were cleared with xylene to remove the ethanol. Following clearance, the tissues were infiltrated with molten paraffin and embedded. All tissue blocks were sectioned into $5 \mu\text{m}$ slices by LEICA RM206. These sections were then stained with hematoxylin and eosin (H & E) for histological observation using an optical microscope (OLYMPUS BX53).

2.4. RNA isolation, cDNA library construction and sequencing

The total RNA of spleen samples was extracted using TRIzol Reagent (Invitrogen, USA). Assess the quantity and quality of isolated RNA through biophotometer (OSTC, China) to measure RNA concentration and agarose gel electrophoresis to check RNA integrity. A total of 12 mRNA sequencing libraries were prepared, with 3 replicate samples collected at each of 4 time points. The libraries were constructed following the protocol of RNA Library Prep Kit (NEB, USA). After quality assessment and quantification, the libraries were subjected to PE150 sequencing on Illumina platforms at Novogene Bioinformatics

Technology Co., Ltd. (Beijing, China).

2.5. Differential expression and functional enrichment analysis

The raw data generated by Illumina platforms were subjected to quality control by FastQC (version 0.11.9). Low-quality sequences and adapters were trimmed by Trimmomatic (version 0.39). Then, clean reads were aligned to spotted sea bass female reference genome (JAYMHB000000000) by Hisat2 (version 2.2.1). Transcript quantification was performed using featureCounts (version 2.0.1) (Liao et al., 2014). Differential expression analysis between the control group and treatment group of each time point was carried out by DESeq2 (version 1.30.1) (Kim et al., 2015), applying a threshold of adjusted p -value < 0.05 and $|\log_2\text{FoldChange}| \geq 1$. Principal component analysis (PCA) was then conducted to analyze the correlation between each samples. KOBAS (<http://kobas.cbi.pku.edu.cn/>) was used to conducted functional enrichment analysis to delineate the potential function of DEGs, applying a threshold of adjusted p -value < 0.05 to filter the significant GO terms and pathways. Ggplot2 v3.35 R package was used to visualized the significant results.

2.6. WGCNA and hub genes identification

Preprocess the gene expression data to remove low-quality reads, normalize expression values, and filter out genes with low expression level (FPKM < 1) and import the genes into WGCNA in R (Langfelder and Horvath, 2008). Samples were clustered to assess the presence of any obvious outliers. We chose the soft-threshold $\beta = 16$ to constructed a scale-free network. Calculated the module eigengene and hierarchically clustered the modules. Performed module-trait correlation analysis to assess the relationship between module eigengenes and traits, and the strongest positive correlation was selected for further analysis. Within significant modules, we identified hub genes based on their intra-modular connectivity, through measuring gene significance (GS) and module membership (MM). Finally, functional enrichment analysis (GO and KEGG pathway) was carried out on genes in the significant modules, with hub genes identified using criteria of $GS > 0.8$ and $MM > 0.8$. The interaction network of hub genes was displayed by Cytoscape (v3.8.2).

2.7. Differential alternative splicing (DAS) events analysis

The rMATS (v.4.01) was used to detect and quantify AS events, including skipped exon (SE), alternative 5' splice site (A5SS), alternative 3' splice site (A3SS), mutually exclusive exons (MXE), and retained intron (RI). Percent Spliced In (PSI) values were calculated for each splicing event. Significant differences in PSI values between different treatment groups were assessed to identify the DAS, applying a threshold of FDR < 0.05 . Functional annotation and enrichment analysis of genes undergoing differential splicing were conducted to understand their biological relevance.

2.8. Real-time RT-PCR verification and statistical analysis

Eight candidate DEGs were randomly chosen for the verification of the RNA-Seq data by RT-qPCR. Specific primers for candidate genes were designed by Primer-BLAST (<https://www.ncbi.nlm.nih.gov/tools/primer-blast/>) (Table S1). 18 s RNA was used as the reference gene to calibrate the RT-qPCR. First-strand cDNA synthesis was performed with SPARKscript II RT Plus Kit (with gDNA Eraser) (Sparkjade, China) according to the protocol. Briefly, RNA was reverse transcribed into cDNA using oligo(dT) primers and reverse transcriptase enzymes. PCR amplification was performed using a thermal cycler with appropriate cycling conditions and the reactions were executed in a StepOne Plus Real-Time PCR system (Applied Biosystems). Each data point was analyzed in triplicate to ensure reproducibility. The $2^{-\Delta\Delta C_t}$ method was used to analyze the relative gene expression level (Livak and Schmittgen,

2001).

3. Results

3.1. Clinical symptoms and histological structures

Upon infection of spotted sea bass with *N. seriolae*, distinct clinical symptoms emerged, including abdominal and anal redness and swelling. Subsequent dissection revealed the congestion in visceral organs, alongside the presence of abundant white nodules on the gill and in visceral mass, particularly on the spleen (Fig. 1). Histological analysis of spleen tissues at 48 h, 96 h, and 120 h post-infection revealed notable alterations in tissue structure. The control group exhibited a healthy spleen with a standard structure (Fig. 2A). At 48 h post-infection, the macrophage and lymphocyte were filtrated into the lesion site (Fig. 2B). And at 96 h post-infection, a thin layer of fibrous connective tissue enveloped the lesion (Fig. 2C). While at 120 h post-infection, the center of the granulomas displayed caseous necrosis, accompanied by a substantial increase in macrophage density within the granuloma center (Fig. 2D).

3.2. The data statistics of transcriptomes

To investigate the transcriptional mechanism of pathogenesis, we constructed 12 cDNA libraries for further sequencing, yielding 547.32 million (547,324,082) raw reads. Following quality filtering, 506.71 million (506,705,872, 92.58%) high-quality clean reads were attained. Approximately 81% of the high-quality clean reads were mapped to spotted sea bass genome (Table S2). The raw RNA-seq data have been submitted to the NCBI Sequence Read Archive (SRA) database

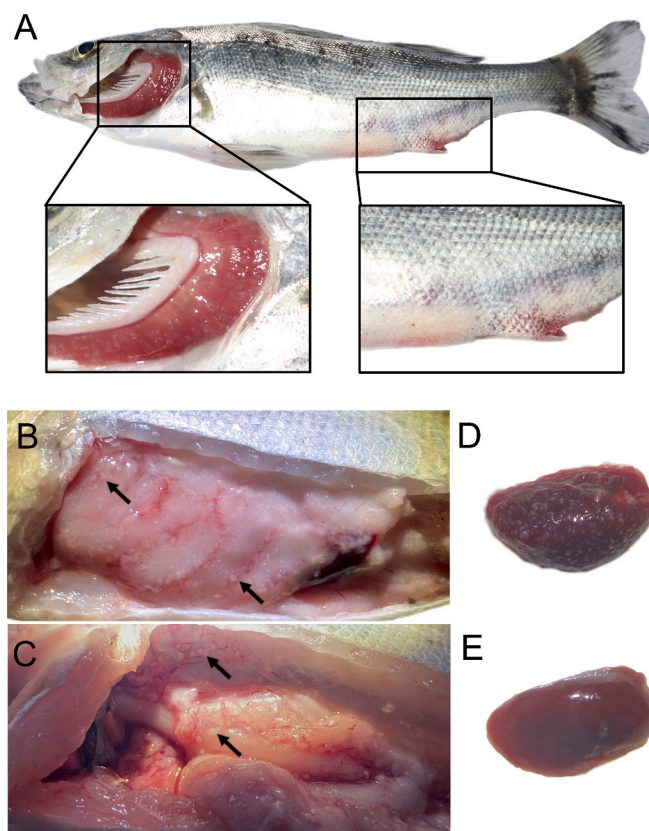


Fig. 1. Clinic symptoms of spotted sea bass infected with *N. seriolae*. Diseased fish showing abdominal and anal redness and swelling. Numerous white nodules on the gill (A), and in visceral mass (B, C). The spleen of infected fish (D) and healthy fish (E).

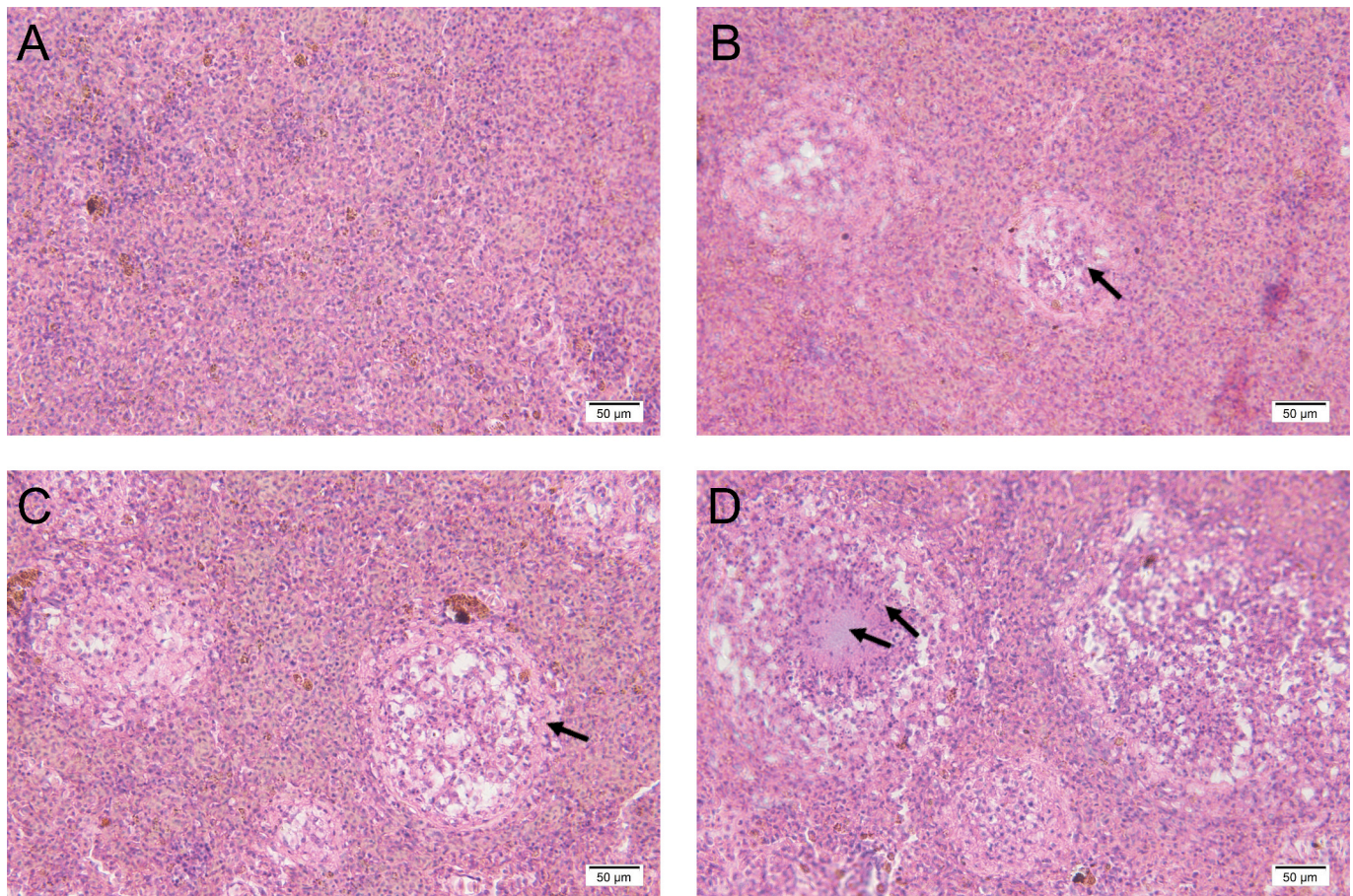


Fig. 2. Histopathological observation of the spleens of spotted sea fish infection with *N.seriolae*. Normal spleen tissue from control group (A); 48 h spleen tissue (B); 96 h spleen tissue (C); 120 h spleen tissue (D). H & E, Bars = 50 µm.

(PRJNA1093234). The PCA revealed distinct clustering of samples into 4 groups, confirming the suitability of the generated sequencing data for subsequent analysis (Fig. S1).

3.3. Identification of DEGs

The expression differences were compared between 48 h, 96 h, 120 h post-*N. seriolae* infection and control group, which generated three comparison groups, including 48 h vs. 0 h, 96 h vs. 0 h and 120 h vs. 0 h. A total of 3031, 3597, and 4683 DEGs were identified in three comparison groups, respectively. A progressive augmentation in the count of DEGs was observed concomitant with the prolonged duration of bacterial challenge. Among these DEGs, there were 1663, 1948, and 2413 upregulated genes were identified in comparison groups of 48 h vs. 0 h, group 96 h vs. 0 h and 120 h vs. 0 h, respectively. Additionally, 1368, 1649 and 2270 downregulated genes were identified in the respective comparison groups (Fig. 3). As illustrated in Venn diagram (Fig. 3D), there is a large quantity of overlapping DEGs, accounting for 2180, between three comparison groups.

3.4. Functional enrichment analysis of DEGs

GO enrichment analysis were carried out to discern the biological functions of overlapping DEGs of three comparison groups. A total of 142 GO terms were found to be significantly enriched in up-regulated overlapping DEGs of three comparison group (Table. S3). More specifically, under the Biological Process category, most of the terms are related to immune, including macrophage chemotaxis, response to bacterium and inflammatory response. Among these, complement

activation has the highest enrichment level. Cytokine binding and cytokine receptor activity were the predominant subcategory within the Molecular Function category (Fig. 4A). By contrast, only 49 GO terms were found to be significantly enriched in down-regulated overlapping DEGs (Table. S3). Under the Biological Process category, the highest enrichment level term was swimming. Besides, some terms related with autophagy were enriched, including autophagy of mitochondrion and autophagosome assembly. Under the Cellular Component category, the highest enrichment level term was Cul4-RING E3 ubiquitin ligase complex. And autophagosome was also involved (Fig. 4B). The DEGs were then subjected to KEGG pathway enrichment analysis. A total of 39 pathways were found to be significantly enriched in up-regulated intersection DEGs of three comparison group (Table S4). Among these pathways, up-regulated DEGs have significant enrichment in immune-related pathways, including C-type lectin receptor signaling pathway, NLR signaling pathway and TLR signaling pathway. Meanwhile, some inflammation related pathways, like Cytokine-cytokine receptor interaction and VEGF signaling pathway, were also identified. Besides, the enrichment of cell cycle and p53 signaling pathway were also identified, which participate in cell growth and death (Fig. 4C). By contrast, only 7 pathways were significantly enriched in down-regulated DEGs, which mainly related to autophagy (Fig. 4D). In order to determine the functional differences between the DEGs in three comparison groups, we also performed KEGG pathway enrichment analysis in each comparison groups, respectively. More specifically, except that pathways mentioned above, we identified Chemokine signaling pathway in 96 h vs. 0 h group. And mTOR signaling pathway and Apoptosis in 120 h vs. 0 h group (Fig. S2).

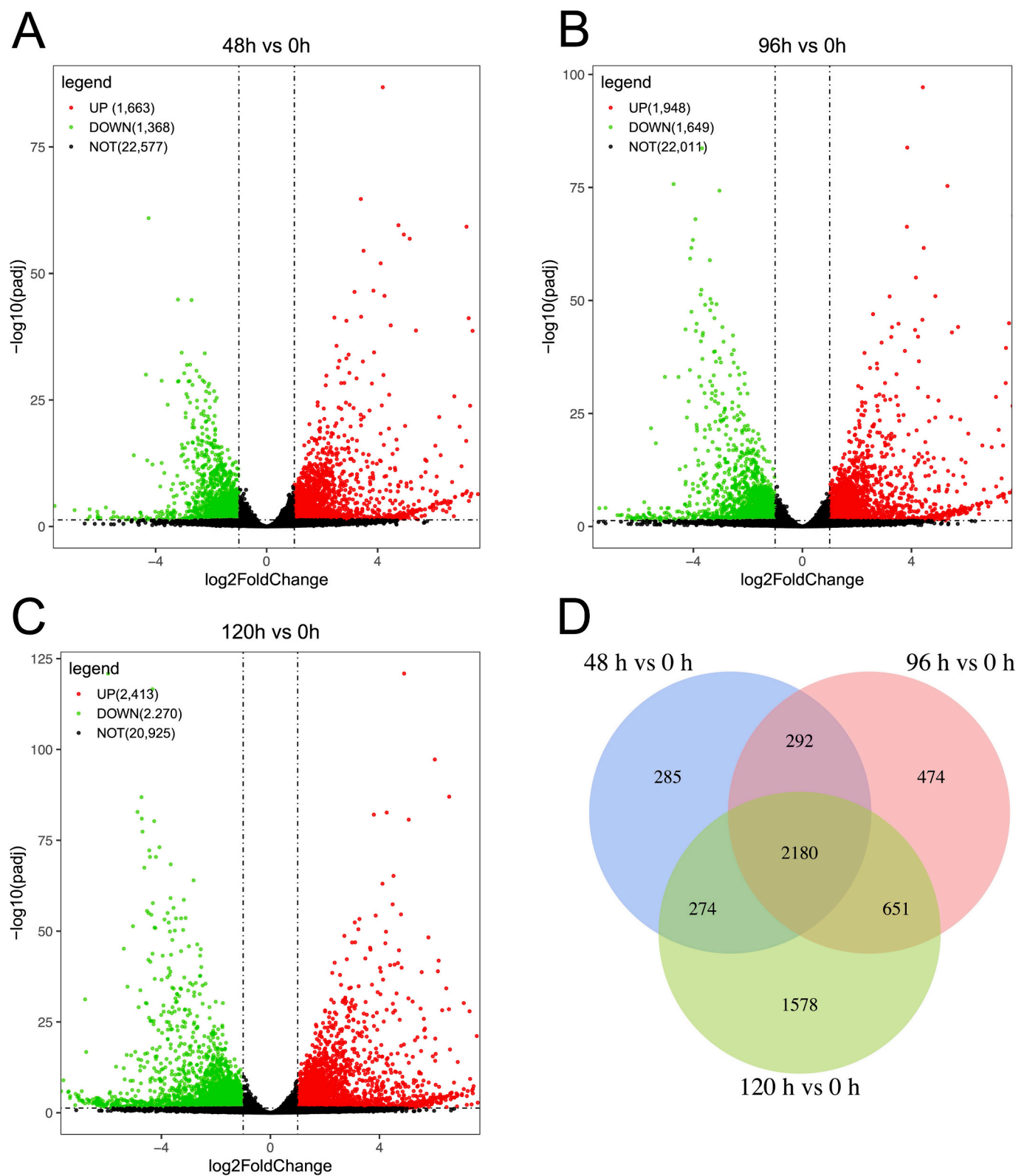


Fig. 3. Volcano plots displayed expression profiling of DEGs between 48 h vs 0 h (A), 96 h vs 0 h (B), 120 h vs 0 h (C), respectively. Red dots represented up-regulated genes, green dots represented down-regulated genes and black dots represented genes with no significant expression differences. The x-axis indicated \log_2 Fold change, and the y-axis indicated $-\log_{10} p$ -value. The number of genes is indicated in parentheses. Venn diagram showing overlapping DEGs at three comparison groups (D). (For interpretation of the references to colour in this figure legend, the reader is referred to the web version of this article.)

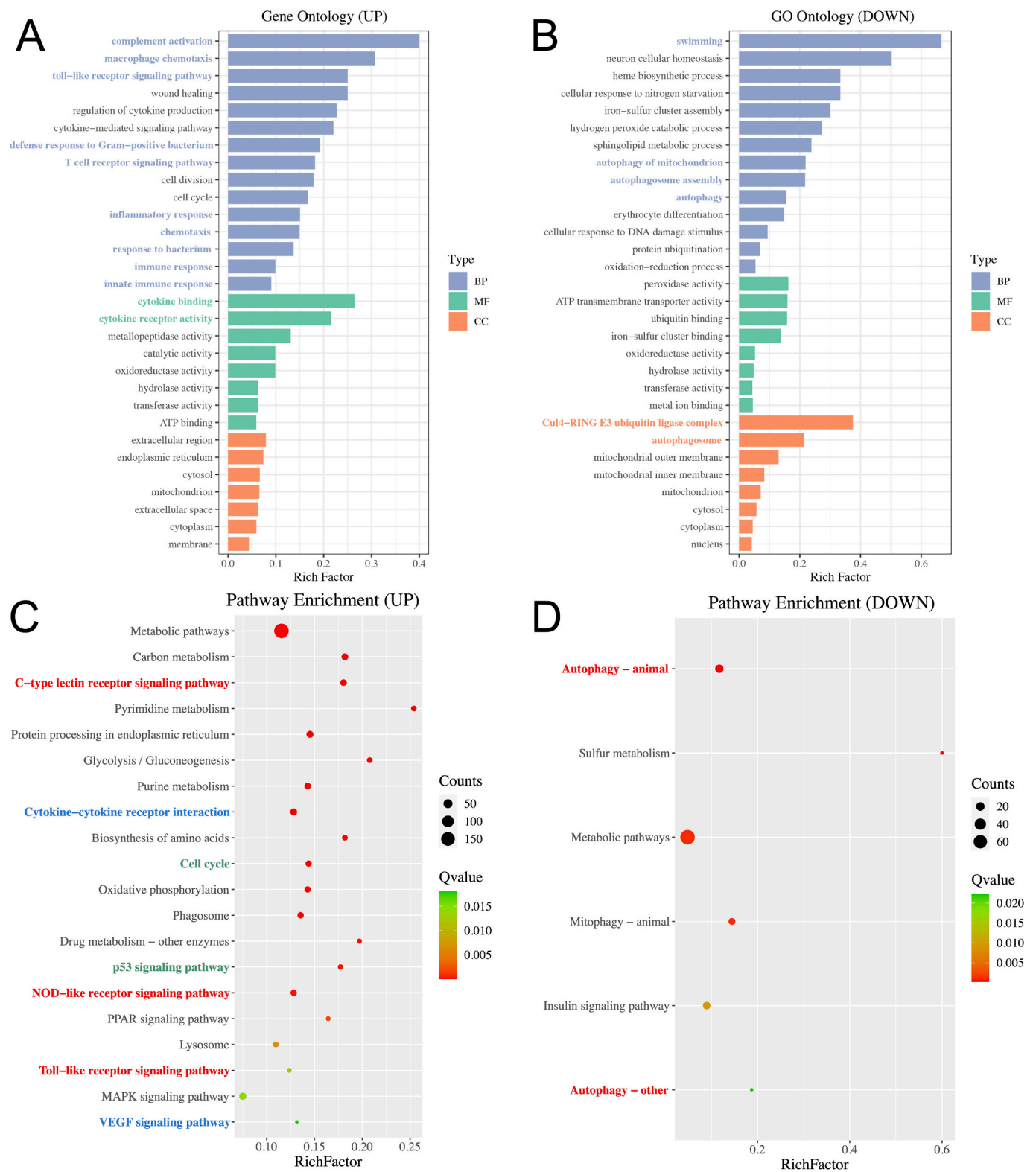


Fig. 4. Functional enrichment analysis of overlapping DEGs. Gene Ontology (GO) annotations analysis of up (A) and down (B) overlapping DEGs. KEGG enrichment analysis of up (C) and down (D) overlapping DEGs.

3.5. Identification of hub genes by WGCNA

The samples were clustered using parson's correlation coefficient, resulting in a dendrogram displaying sample-trait relationships (Fig. 5A). To constructed a scale-free network, a soft thresholding parameter $\beta = 16$ was selected (Fig. 5B, C). A total of 11 modules were

identified shown in hierarchical cluster dendrogram (Fig. 5D). To identified the key module related to *N.seriolae* infection, the correlation between the modules and the phenotype traits was investigated. We found that the blue module emerged as the most highly correlated with pathogenic infections (correlation coefficient = 0.95, $p = 2e-6$) (Fig. 5E). The blue module contains 2090 genes, of which 449 genes were

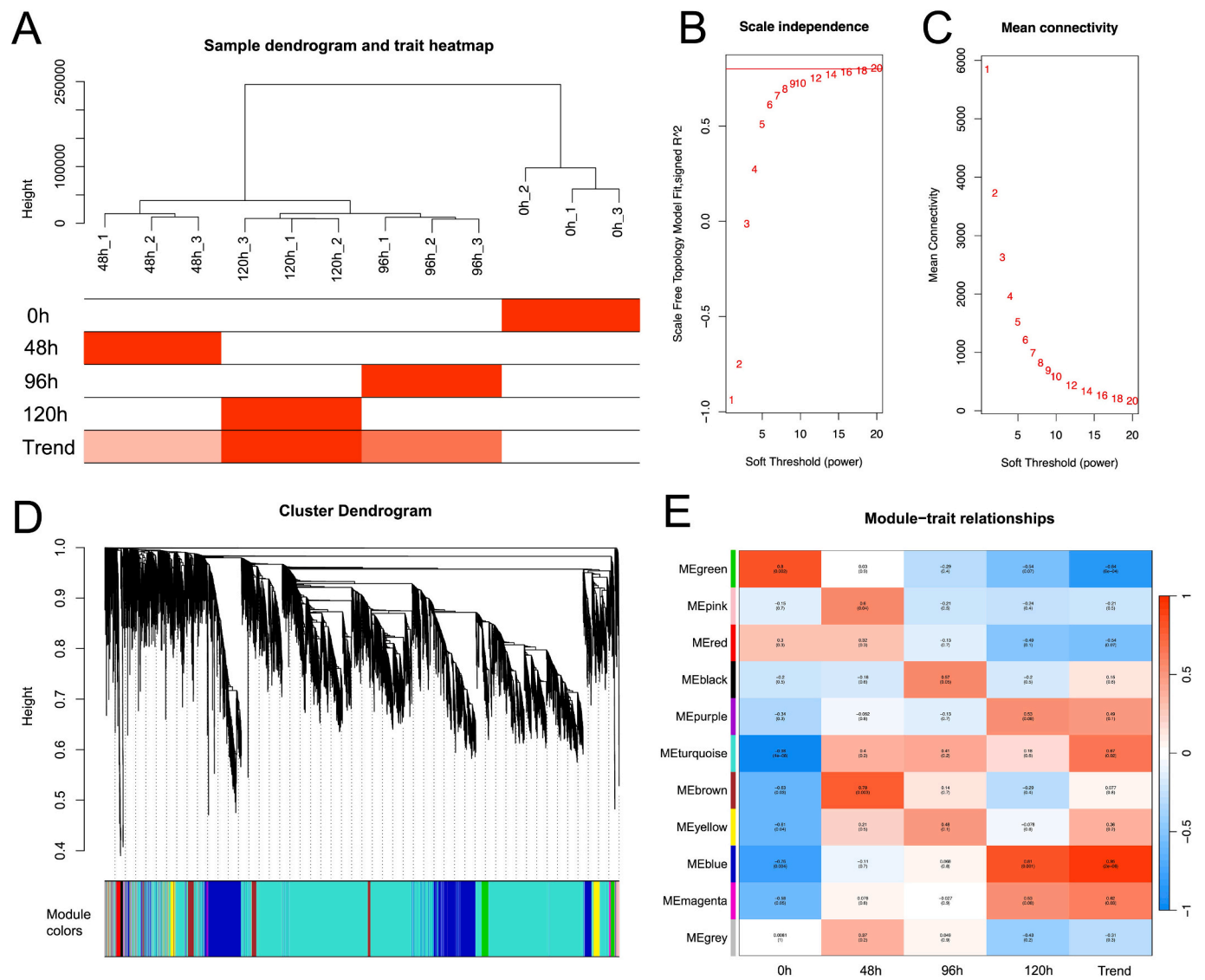


Fig. 5. The co-expression modules analysis. Clustering dendrogram of samples (A); The relationship between the scale-free fit index and various soft-threshold powers (B); The relationship between the mean connectivity and various soft-threshold powers (C); Cluster dendrogram of genes in the co-expression network, different colors represent different modules (D). The relationship of 11 modules and traits (E).

identified as core genes with $MM > 0.9$ and $GS > 0.9$ (Fig. 6A). KEGG enrichment analysis suggested the enrichment of immune-related pathways within the core genes, including Ferroptosis, Necroptosis and TLR signaling pathway (Fig. 6B). A PPI network of top 10 hub genes form 449 core genes were analyzed and constructed using the Cytoscape plugins (CytoHubba) (Fig. 6C).

3.6. Identification of DAS events and DAS genes

Alternative splicing analysis identified a total of 114, 103 and 113 DAS events in 48 h vs. 0 h, 96 h vs. 0 h and 120 h vs. 0 h, respectively. Among these events, SE was the most prevalent, constituting approximately 51%, while A3SS was the least common, constituting approximately 2% (Fig. 7A). Fifteen genes exhibited alternative splicing across all comparison groups, including *mif* (macrophage migration inhibitory factor) and *LOC111227158* (cell death-inducing p53-target protein 1 homolog) (Fig. 7B). In order to reveal the potential function of DAS genes, all the DAS genes were subjected to KEGG enrichment analysis. A total of 23 pathways were significantly enriched, including RIG-I-like receptor signaling pathway, p53 signaling pathway and Autophagy- other, and some pathways related genetic information Processing like

Nucleotide excision repair (Fig. 7C).

3.7. Verification of RNA-seq data by RT-qPCR

To validate the RNA-seq results, eight DEGs were randomly chosen for RT-qPCR. The expression patterns of all selected DEGs exhibited concordance with the RNA-seq data, with $R^2 = 0.966$ (Fig. S3). Overall, the congruence between the RNA-seq and qPCR outcomes underscores the dependability and precision of the RNA-seq analysis.

4. Discussion

Aquaculture, as a mean of supplying food and protecting fishery resources, has important strategic significance. However, the frequent outbreaks of bacterial diseases have significantly hindered aquaculture development and caused substantial economic losses (Frans et al., 2011; Teng et al., 2022; Zapata et al., 2006). Among these diseases, fish nocardiosis caused by *N. seriolae* emerges as the most prevalent bacterial diseases in spotted sea bass, which is characterized by numerous white or grey nodules on gill and in visceral mass (Maekawa et al., 2018). There is still limited research on the molecular mechanism of immune

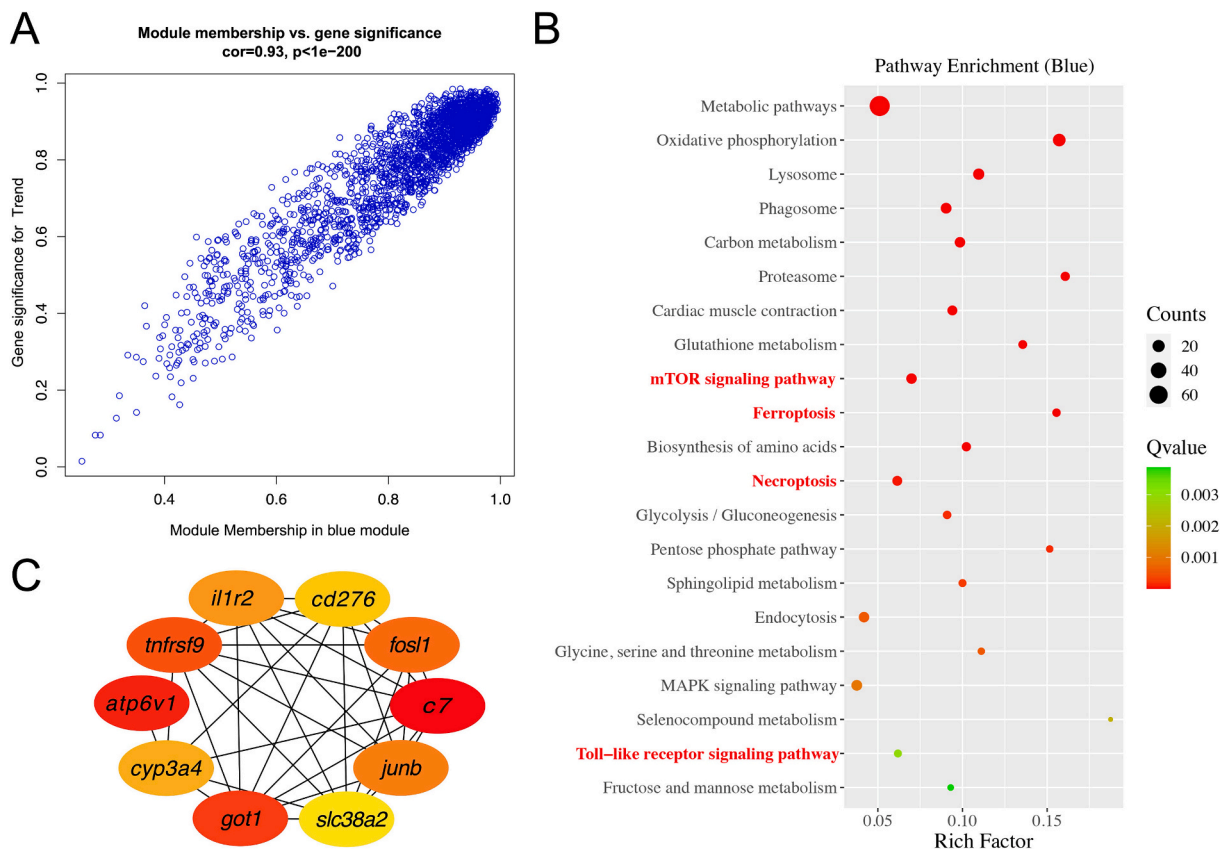


Fig. 6. Screening of hub-genes related to the immune response in blue module. The scatterplot describing the relationship between MM and GS in green module (A); KEGG enrichment analysis of genes in blue module (B); The PPI network of top 10 hub-genes in blue module analyzed by cutyHubba software (C). (For interpretation of the references to colour in this figure legend, the reader is referred to the web version of this article.)

response against to pathogens on spotted sea bass. Thus, in this study, to provide a comprehensive view of the immune response against *N. seriolae* infection, transcriptome analysis was performed on the spleen, one of the fish immunocompetent organs (Zapata et al., 2006), to investigate the regulatory mechanism and the expression of core immune genes.

The innate immune system of fish recognizes pathogens through PRRs in order to trigger the immune cascade. TLR5, a kind of membrane-bound signaling PRRs, have been proved that had specific binding capacity to bacteria and exhibited strong expression at 10 h–16 h after *V. alginolyticus* infection in teleost (Wang et al., 2016; Zhu et al., 2020). TLR signaling pathway has been significantly enriched at 48 h after pathogens invasion on snakeheads and silver pomfret (*Pampus argenteus*) (Nawaz et al., 2022; Teng et al., 2022). A broad repertoire of CTLs have been identified and functional indicated in teleost, such as blunt snout bream (*Megalobrama amblycephala*) (Liu et al., 2023b), large yellow croaker (Lv et al., 2016) and spotted knifejaw (*Oplegnathus punctatus*) (Liu et al., 2019). Notably, CTLs were able to activate the complement system and participate in the immune response to against pathogens infections in roughskin sculpin (*Rachidermus fasciatus*) (Yu et al., 2020). Unlike TLRs and CTLs, researches on NLRs were limited in teleost. NOD1 and NOD2 have been demonstrated that could identify the bacterial components and its degraded products and then initiate the NF-κB signaling pathway, inducing inflammatory response in teleost (Bi et al., 2017; Bi et al., 2018; Swain et al., 2013). In our study, a large quantity of overlapping up-regulation DEGs among three comparison groups were identified, with enrichment in TLR receptor signaling pathway, NLR signaling pathway and C-type lectin receptor signaling pathway. Besides, we identified some PPRs like *tlr5* and *clec1b* exhibited significantly upregulated at the comparison group of 120 h vs. 0 h with fold-change of 4.74 and 6.28, respectively. Our findings indicated that the PPRs of spotted sea bass could participated in recognizing and combating *N.*

seriolae invasion, and *N. seriolae* infection could upregulate the genes involved in these pathways and activate the innate immunity of spotted sea bass throughout the course of infection.

Previous studies have showed that PRRs identify the invading pathogens, initiating the signaling cascades to activate the innate immunity by stimulating various downstream signaling molecules, most of which are cytokines, and even directed the appropriate adaptive immune response (Kawai and Akira, 2010; Thaiss et al., 2016). As is widely known, tumor necrosis factor (TNF), interleukins (IL) and chemokines are typical cytokines. In our investigation, we revealed the enrichment of up-regulated DEGs in the Cytokine-cytokine receptor interaction pathway. Notably, many cytokines-related DEGs were involved in this pathway. The TNF superfamily are known for their ability to bind to specific receptors on the cell surface, triggering intracellular signaling cascades that modulate cellular responses, like inflammation. TNFRSF9, as a member of these superfamily, could activate signaling pathways like NF-κB, AKT, p38 and MAPK to promote cell survival and participate in inflammation in human diseases (Jung et al., 2004). So far, the reports about TNFRSF9 in fish are still lack. It has been reported that rainbow trout (*Oncorhynchus mykiss*) *tnfrsf9* could be significantly up-regulated after *F. psychrophilum* infection (Kutyrev et al., 2016). Interleukin-1 receptor type II (IL1R2) has been identified in some teleost, like rainbow trout (Sangrador-Vegas et al., 2000), Japanese flounder (*Paralichthys olivaceus*) (Fan et al., 2010) and seabream (*Sparus aurata*) (López-Castejón et al., 2007). Researches in Atlantic salmon (*Salmo salar*) showed that IL-1R2 was up-regulated after *Vibrio anguillarum* infection (Stansberg et al., 2005). In this study, *thfrsf9* and *ilr2* have both been identified that significantly upregulated at all time points. Furthermore, they were also identified as two of the ten hub genes in blue module identified by WGCNA, which means they were highly associated with *N. seriolae* infection. Chemokines could guide immune cells to the sites of

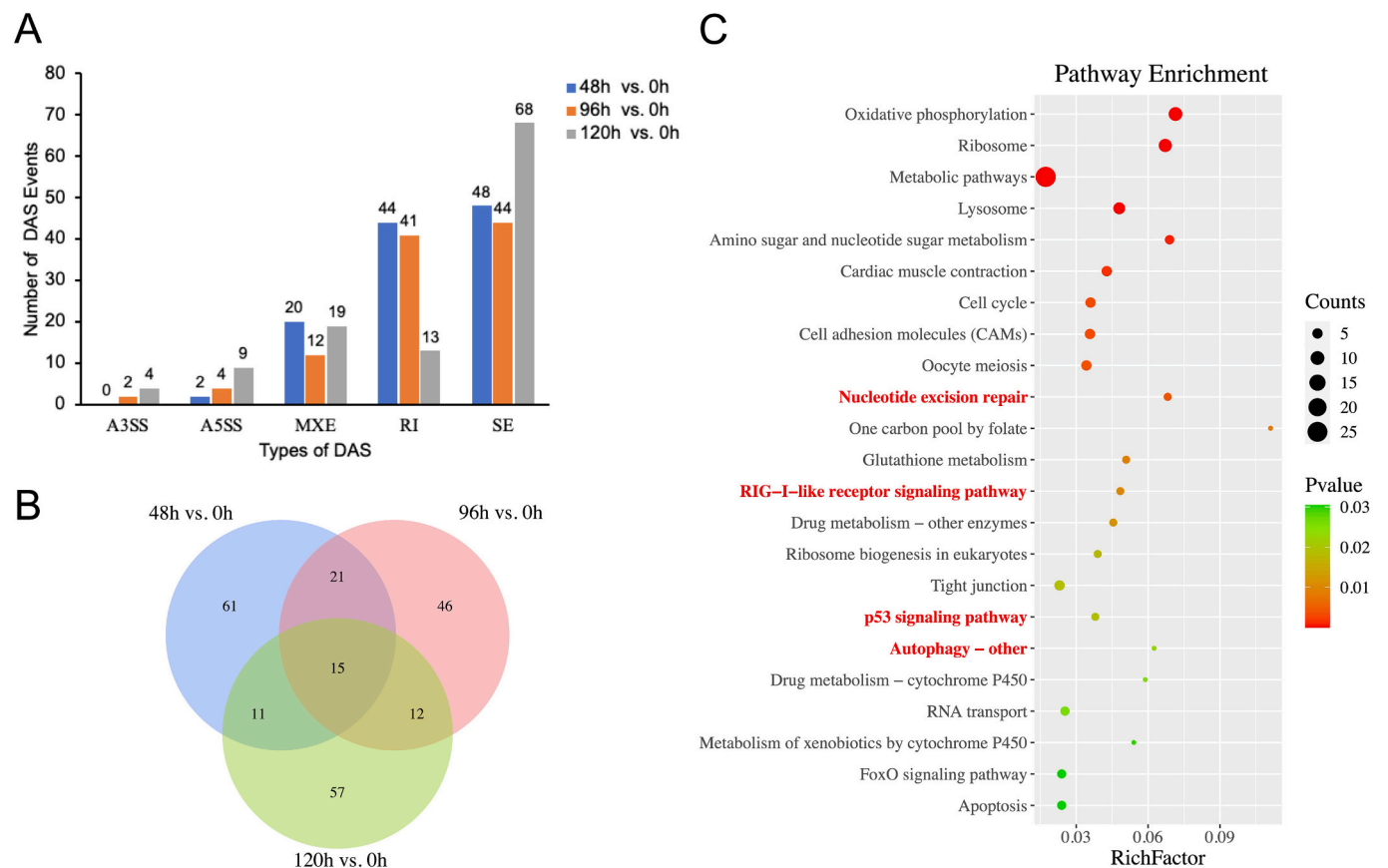


Fig. 7. The profiles of DAS events. The number of DAS events in three comparison groups (A); Venn diagram showing overlapping DAGs at three comparison groups (B). KEGG enrichment analysis of DAS genes (C).

inflammation and arrange communications between immune cells, bridging innate and adaptive immunity(Sokol and Luster, 2015). In our study, Chemokine signaling pathway were investigated the enrichment in the 96 h vs. 0 h group, with several chemokine genes such as *cxcl8*, *cxcl12*, *cxcr3*, *ccl8* and *ccl19* significantly up-regulated, particularly

ccl19 exhibiting a maximum fold-change of 4.76 at 48 h vs. 0 h group. Taken together, our results suggest that invading *N.seriolae* would be recognized by PPRs like TLRs, NLRs and CLRs in spotted sea bass, leading to the secretion of cytokines regulated by genes like *thfsf9*, *ilr2*, *cxcl* and *ccl* to activate both innate and adaptive immunity. The secretion

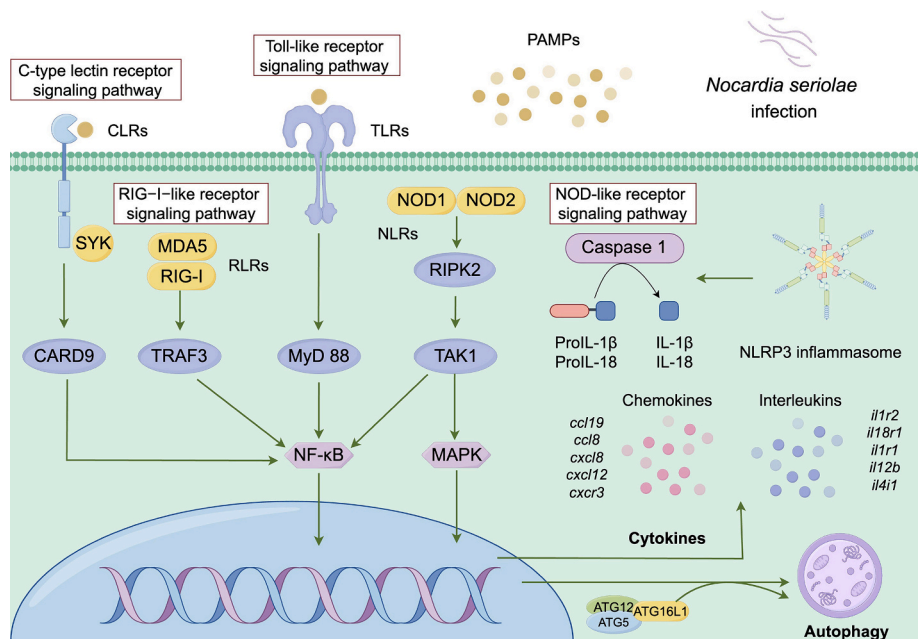


Fig. 8. Schematic regulatory network of immune response in spotted sea bass infected with *N. seriolae* using Figdraw (www.figdraw.com).

of a series of chemokines might guide some inflammation factors to surround the lesions and result in the formation of granuloma in visceral mass of spotted sea bass (Fig. 8).

The complement system has a sophisticated linkage in bridging innate and adaptive immunity in teleost (Nakao et al., 2011). While the mammalian complement system consist a wide variety of types, only a few complement proteins have been recognized in teleost and are homologues to their mammalian equivalents (Schmidt et al., 2016). Initiation of the complement system cascade resulting in formatting the membrane attack complex (MAC). C7 with other lytic complement participated in the assemble of MAC, which can insert into target cell membrane, aiding in host defense against pathogens while also contributing to the promotion of inflammation (Bossi et al., 2009). The expressions of *c7* were significantly changed after bacteria challenge in fish including grass carp (*Müchthys müiy*) and müiy croaker (*Ctenopharyngodon idella*) (Shen et al., 2012; Wang et al., 2015). In our study, we observed that up-regulated genes were notably enriched in the complement activation term. Meanwhile *c7* gene was also differently expressed after *N.seriolae* infection, showing a continuous increase throughout the infection process. Besides, we identified *c7* as a hub gene within the blue module was positive correlated with *N.seriolae* infection trait.

The VEGF signaling pathway is intricately involved in numerous ligand–receptor interactions that orchestrates various processes (Penn et al., 2008). VEGF, known as a multifunctional angiogenic regulator, is capable of stimulating epithelial cell proliferation and promoting blood vessel formation. It also has been characterized as a vascular permeability factor due to its capacity of inducing tissue edema (Lee et al., 2004). It has been proved that VEGF-A activated VEGF receptor2 tyrosine kinase, inducing angiogenesis and increase vascular permeability (Peach et al., 2018). Vascular barrier could significantly influence the containment of antigen spreading and inflammation. Intestine vascular barrier dysfunction will lead to intestine inflammation. In this study, we observed enrichment of VEGF signaling pathway in up-regulated genes. And we found that spotted sea bass infected with *N.seriolae* exhibited severe intestine inflammation. Therefore, *N.seriolae* infection may impair the intestine barrier and induce an increase in inflammatory cytokines, activating the VEGF signaling pathway, which induces angiogenesis and increases vascular permeability.

mTOR orchestrates the assembly of two distinct complexes, mTORC1 and mTORC2, to regulate various progresses, including autophagy (Laplanche and Sabatini, 2012). Autophagy acts as a means to eliminate misfolded proteins and dysfunctional organelles, which is also a way to clear invading pathogens (Morishita and Mizushima, 2019). During cellular stress when mTORC1 is inactive, autophagy will be initiated (Dossou and Basu, 2019). Researches show that autophagy related genes were up-regulated after pathogens invasion in fish (Nombela et al., 2019; Wang et al., 2021). Contrary to prevailing research findings, our investigation reveals a divergence. Notably, genes up-regulated in the 120 h vs. 0 h comparison group exhibit enrichment in the mTOR signaling pathway, while down-regulated genes manifest enrichment in several autophagy-related pathways and GO terms. This incongruity prompts a deeper exploration. Studies showed that the transcription factor p53 intertwines with autophagy through mTOR inhibition (Feng et al., 2005), while in other study, cytoplasmic p53 was able to repress the autophagy (Tasdemir et al., 2008). The p53 and autophagy are functionally intertwined. Recently, studies in large yellow croaker showed that the involvement of a *cd82a*-mediated p53 signaling pathway activation in response to VWND (Bai et al., 2022). Remarkably, our findings unveil that the up-regulated overlapping genes are also enriched in the p53 signaling pathway. In light of our study, it is plausible to infer that when faced with an overwhelming barrage of pathogens, the cellular milieu succumbs to external pressures, surpassing its coping capacity. The down-regulation of autophagy-related genes leaves the organism bereft of its intrinsic defense mechanisms, thereby setting the stage for the activation of programmed cell death pathways.

Simultaneously, the suppression of key autophagic genes such as *atg101* and *bcl1* culminates in the paralysis of the autophagy program, unraveling the cell's innate self-protective mechanisms. These findings underscore the intricate balance between autophagy, apoptosis, and pathogen-induced cellular responses, thereby enriching our comprehend of host-pathogen interactions at the molecular level.

In the intricate landscape of host-pathogen interactions, alternative splicing emerges as a pivotal regulatory mechanism orchestrating immune responses against pathogen infection. The DAS genes of large yellow croaker infected with *Cryptocoryn irritans* were predominantly enriched in immune related pathways (Qu et al., 2022). Similarly, studies in tongue sole (*Cynoglossus semilaevis*) unveiled the participation of DAS events in the immune response after *Vibrio anguillarum* infection, and they also found two isoforms of *hp* genes to exert divergent effects on the expression of immune factors (Han et al., 2024). In our investigation, we discern that DAS genes were significantly enriched in RIG-I-like receptor signaling pathway. In aquatic animals, RLRs exhibit structural and functional diversity including RIG-I, MDA5, and LGP2, each exerting differential regulatory effects on the expression of IFNs. (Liang and Su, 2021). For instance, RIG-Ib notably potentiates the activation of IFN promoter, whereas RIG-Ia remains inert in zebrafish. Similarly, zebrafish MDA5a emerges as a potent inducer of IFN promoter activation, outstripping the efficacy of MDA5b (Zou et al., 2015; Zou et al., 2014). Trout LGP2a plays a positive regulatory role in antiviral response, while LGP2b exerts a negative regulatory effect on the antiviral signal transduction induced by LGP2a by competing with viral RNA PAMP (Chang et al., 2011). Overall, different isoforms may have different functions to regulated the expression of downstream genes. Our study uncovered the possibility that genes involved in the RIG-I-like receptor signaling pathway may have different isoforms, ultimately shaping immune responses against *N.seriolae* infection in spotted sea bass. In addition, we also found a cadre of immune-related genes within the DAS gene set, including E3 ubiquitin-protein ligase genes, C-type lectin domain-containing protein (*clc4c*), *mif*, and *LOC111227158*, which indicated that their plausible role in orchestrating responses to *N. seriolae* infection in spotted sea bass and AS played an important roles under various immune related responses, like proteolysis pathways, cell apoptosis and the activation of innate and adaptive immunity.

In summary, in our current investigation, the pathogenic bacterium *N.seriolae* caused the formation of numerous white or grey nodules on gills and in visceral mass. The histological analysis showed the structural changes of the spleen after *N.seriolae* infection in different stages. We provided a time series of gene expression profiles within the spleen of spotted sea bass after *N.seriolae* infection, along with their involved signaling pathway. We identified 10 pivotal immune-related hub genes by WGCNA. We carried out the AS analysis to investigate the potential impact of DAS events on immune response. These results offer novel insights to the molecular regulatory mechanism governing the immune response against *N.seriolae* invasion, and lay a foundational framework endeavor aimed at breeding spotted sea bass endowed with heightened disease resistance.

Supplementary data to this article can be found online at <https://doi.org/10.1016/j.aquaculture.2024.741178>.

CRedit authorship contribution statement

Yani Dong: Writing – original draft, Visualization, Investigation, Formal analysis. **Haishen Wen:** Resources, Conceptualization. **Yong-hang Zhang:** Visualization. **Xin Qi:** Resources, Conceptualization. **Lingyu Wang:** Visualization. **Hao Li:** Visualization, Resources. **Kai-qiang Zhang:** Resources, Methodology. **Yun Li:** Writing – review & editing, Supervision, Methodology, Funding acquisition.

Declaration of competing interest

The authors declare that they have no known competing financial

interests or personal relationships that could have appeared to influence the work reported in this paper.

Data availability

Data will be made available on request.

Acknowledgments

This investigation was supported by National Key Research and Development Program of China [grant number: 2022YFD2400503], National Natural Science Foundation of China [grant number: NSFC, 32072947], and Agriculture Research System of China (CARS for Marine Fish Culture Industry) [grant number: CARS-47].

References

- Acosta, F., Vega, B., Monzón-Atienza, L., Superio, J., Torrecillas, S., Gómez-Mercader, A., Castro, P., Montero, D., Galindo-Villegas, J., 2024. Phylogenetic reconstruction, histopathological characterization, and virulence determination of a novel fish pathogen, *Nocardia brasiliensis*. *Aquaculture* 581, 740458. <https://doi.org/10.1016/j.aquaculture.2023.740458>.
- Bai, Y., Qu, A., Liu, Y., Chen, X., Wang, J., Zhao, J., Ke, Q., Chen, L., Chi, H., Gong, H., Zhou, T., Xu, P., 2022. Integrative analysis of GWAS and transcriptome reveals p53 signaling pathway mediates resistance to visceral white-nodules disease in large yellow croaker. *Fish Shellfish Immunol.* 130, 350–358. <https://doi.org/10.1016/j.fsi.2022.09.033>.
- Bi, D., Gao, Y., Chu, Q., Cui, J., Xu, T., 2017. NOD1 is the innate immune receptor for iE-DAP and can activate NF- κ B pathway in teleost fish. *Dev. Comp. Immunol.* 76, 238–246. <https://doi.org/10.1016/j.dci.2017.06.012>.
- Bi, D., Wang, Y., Gao, Y., Li, X., Chu, Q., Cui, J., Xu, T., 2018. Recognition of lipopolysaccharide and activation of NF- κ B by cytosolic sensor NOD1 in teleost fish. *Front. Immunol.* 9, 1413. <https://doi.org/10.3389/fimmu.2018.01413>.
- Bossi, F., Rizzi, L., Bulla, R., Debeus, A., Tripodo, C., Picotti, P., Betto, E., Macor, P., Pucillo, C., Würzner, R., Tedesco, F., 2009. C7 is expressed on endothelial cells as a trap for the assembling terminal complement complex and may exert anti-inflammatory function. *Blood* 113 (15), 3640–3648. <https://doi.org/10.1182/blood-2008-03-146472>.
- Buchmann, K., 2014. Evolution of innate immunity: clues from invertebrates via fish to mammals. *Front. Immunol.* 5, 459. <https://doi.org/10.3389/fimmu.2014.00459>.
- Chang, M., Collet, B., Nie, P., Lester, K., Campbell, S., Secombes, C.J., Zou, J., 2011. Expression and functional characterization of the RIG-I-like receptors MDA5 and LGP2 in rainbow trout (*Oncorhynchus mykiss*). *J. Virol.* 85 (16), 8403–8412. <https://doi.org/10.1128/jvi.00445-10>.
- Chen, S.-C., Lee, J.-L., Lai, C.-C., Gu, Y.-W., Wang, C.-T., Chang, H.-Y., Tsai, K.-H., 2000. Nocardiosis in sea bass, *Lateolabrax japonicus*, in Taiwan. *J. Fish Dis.* 23 (5), 299–307. <https://doi.org/10.1046/j.1365-2761.2000.00217.x>.
- Chen, Y., Wu, X., Lai, J., Liu, Y., Song, M., Li, F., Gong, Q., 2023. Transcriptome sequencing of the spleen of the Yangtze sturgeon (*Acipenser dabryanus*) under Edwardsiella tarda and poly(I:C) treatments. *Aquac. Reports* 28, 101442. <https://doi.org/10.1016/j.aqrep.2022.101442>.
- Dossou, A.S., Basu, A., 2019. The emerging roles of mTORC1 in macromanaging autophagy. *Cancers (Basel)* 11 (10). <https://doi.org/10.3390/cancers11101422>.
- Fan, Y., Li, S., Qi, J., Zeng, L., Zhong, Q., Zhang, Q., 2010. Cloning and characterization of type II interleukin-1 receptor cDNA from Japanese flounder (*Paralichthys olivaceus*). *Comp. Biochem. Physiol. B Biochem. Mol. Biol.* 157 (1), 59–65. <https://doi.org/10.1016/j.cbpb.2010.05.001>.
- Feng, Z., Zhang, H., Levine, A.J., Jin, S., 2005. The coordinate regulation of the p53 and mTOR pathways in cells. *Proc. Natl. Acad. Sci. USA* 102 (23), 8204–8209. <https://doi.org/10.1073/pnas.0502857102>.
- Frans, I., Michiels, C.W., Bossier, P., Willems, K.A., Lievens, B., Rediers, H., 2011. *Vibrio anguillarum* as a fish pathogen: virulence factors, diagnosis and prevention. *J. Fish Dis.* 34 (9), 643–661. <https://doi.org/10.1111/j.1365-2761.2011.01279.x>.
- Han, S., Tan, S., Liu, H., Wang, N., Liu, X., Li, Z., Wu, Z., Ma, J., Wang, W., Shi, K., Sha, Z., 2024. Analysis of alternative splicing provides insights into its vital roles in immune responses of half-smooth tongue sole (*Cynoglossus semilaevis*) against vibrio anguillarum. *Aquaculture* 582, 740526. <https://doi.org/10.1016/j.aquaculture.2023.740526>.
- Hou, X., Shi, H., Jiang, Y., Li, X., Chen, K., Li, Q., Liu, R., 2023. Transcriptome analysis reveals the neuroactive receptor genes response to Streptococcus agalactiae infection in tilapia, *Oreochromis niloticus*. *Fish & Shellfish Immunol.* 141, 109090. <https://doi.org/10.1016/j.fsi.2023.109090>.
- Jung, H.W., Choi, S.W., Choi, J.I., Kwon, B.S., 2004. Serum concentrations of soluble 4-1BB and 4-1BB ligand correlated with the disease severity in rheumatoid arthritis. *Exp. Mol. Med.* 36 (1), 13–22. <https://doi.org/10.1038/emmm.2004.2>.
- Kawai, T., Akira, S., 2010. The role of pattern-recognition receptors in innate immunity: update on toll-like receptors. *Nat. Immunol.* 11 (5), 373–384. <https://doi.org/10.1038/ni.1863>.
- Kim, D., Langmead, B., Salzberg, S.L., 2015. HISAT: a fast spliced aligner with low memory requirements. *Nat. Methods* 12 (4), 357–360. <https://doi.org/10.1038/nmeth.3317>.
- Kim, Y.K., Shin, J.-S., Nahm, M.H., 2016. NOD-like receptors in infection, immunity, and diseases. *Yonsei Med. J.* 57 (1), 5–14.
- Kraemer, S.A., Ramachandran, A., Perron, G.G., 2019. Antibiotic pollution in the environment: from microbial ecology to public policy. *Microorganisms* 7 (6). <https://doi.org/10.3390/microorganisms7060180>.
- Kutyrev, I., Cleveland, B., Leeds, T., Wiens, G.D., 2016. Proinflammatory cytokine and cytokine receptor gene expression kinetics following challenge with Flavobacterium psychrophilum in resistant and susceptible lines of rainbow trout (*Oncorhynchus mykiss*). *Fish Shellfish Immunol.* 58, 542–553. <https://doi.org/10.1016/j.fsi.2016.09.053>.
- Langfelder, P., Horvath, S., 2008. WGCNA: an R package for weighted correlation network analysis. *BMC Bioinform.* 9, 559. <https://doi.org/10.1186/1471-2105-9-559>.
- Laplanche, M., Sabatini, D.M., 2012. mTOR signaling in growth control and disease. *Cell* 149 (2), 274–293. <https://doi.org/10.1016/j.cell.2012.03.017>.
- Lee, C.G., Link, H., Baluk, P., Homer, R.J., Chapoval, S., Bhandari, V., Kang, M.J., Cohn, L., Kim, Y.K., McDonald, D.M., Elias, J.A., 2004. Vascular endothelial growth factor (VEGF) induces remodeling and enhances TH2-mediated sensitization and inflammation in the lung. *Nat. Med.* 10 (10), 1095–1103. <https://doi.org/10.1038/nm1105>.
- Levine, B., Kroemer, G., 2019. Biological functions of autophagy genes: a disease perspective. *Cell* 176 (1–2), 11–42. <https://doi.org/10.1016/j.cell.2018.09.048>.
- Li, X., Yuan, S., Sun, Z., Lei, L., Wan, S., Wang, J., Zou, J., Gao, Q., 2020. Gene identification and functional analysis of peptidoglycan recognition protein from the spotted sea bass (*Lateolabrax maculatus*). *Fish Shellfish Immunol.* 106, 1014–1024. <https://doi.org/10.1016/j.fsi.2020.08.041>.
- Liang, B., Su, J., 2021. Advances in aquatic animal RIG-I-like receptors. *Fish Shellfish Immunol. Rep.* 2, 100012. <https://doi.org/10.1016/j.fsi.2021.100012>.
- Liao, Y., Smyth, G.K., Shi, W., 2014. featureCounts: an efficient general purpose program for assigning sequence reads to genomic features. *Bioinformatics* 30 (7), 923–930. <https://doi.org/10.1093/bioinformatics/btt656>.
- Liu, W., Deng, Y., Tan, A., Zhao, F., Chang, O., Wang, F., Lai, Y., Huang, Z., 2023a. Intracellular behavior of Nocardia seriolae and its apoptotic effect on RAW264.7 macrophages. *Front. Cell. Infect. Microbiol.* 13, 1138422. <https://doi.org/10.3389/fcimb.2023.1138422>.
- Liu, X., Li, X., Peng, M., Wang, X., Du, X., Meng, L., Zhai, J., Liu, J., Yu, H., Zhang, Q., 2019. A novel C-type lectin from spotted knifejaw, *Oplegnathus punctatus* possesses antibacterial and anti-inflammatory activity. *Fish Shellfish Immunol.* 92, 11–20. <https://doi.org/10.1016/j.fsi.2019.05.054>.
- Liu, Y., Wang, Z., Wang, W., Liu, B., Li, C., Sun, Y., Cao, J., Xia, K., Yang, M., Yan, J., 2023b. Characterization and functional analysis of a novel C-type lectin in blunt snout bream (*Megalobrama amblycephala*). *Fish Shellfish Immunol.* 140, 108966. <https://doi.org/10.1016/j.fsi.2023.108966>.
- Livak, K.J., Schmittgen, T.D., 2001. Analysis of relative gene expression data using real-time quantitative PCR and the 2(-Delta Delta C(T)) method. *Methods* 25 (4), 402–408. <https://doi.org/10.1006/meth.2001.1262>.
- López-Castejón, G., Sepulcre, M.P., Roca, F.J., Castellana, B., Planas, J.V., Meseguer, J., Mulero, V., 2007. The type II interleukin-1 receptor (IL-1RII) of the bony fish gilthead seabream *Sparus aurata* is strongly induced after infection and tightly regulated at transcriptional and post-transcriptional levels. *Mol. Immunol.* 44 (10), 2772–2780. <https://doi.org/10.1016/j.molimm.2006.10.027>.
- Lv, C., Zhang, D., Wang, Z., 2016. A novel C-type lectin, Nattectin-like protein, with a wide range of bacterial agglutination activity in large yellow croaker *Larimichthys crocea*. *Fish Shellfish Immunol.* 50, 231–241. <https://doi.org/10.1016/j.fsi.2016.01.032>.
- Maekawa, S., Yoshida, T., Wang, P.-C., Chen, S.-C., 2018. Current knowledge of nocardiosis in teleost fish. *J. Fish Dis.* 41 (3), 413–419. <https://doi.org/10.1111/jfd.12782>.
- Maiuri, M.C., Zalckvar, E., Kimchi, A., Kroemer, G., 2007. Self-eating and self-killing: cross-talk between autophagy and apoptosis. *Nat. Rev. Mol. Cell Biol.* 8 (9), 741–752. <https://doi.org/10.1038/nrm2239>.
- Morishita, H., Mizushima, N., 2019. Diverse cellular roles of autophagy. *Annu. Rev. Cell Dev. Biol.* 35 (1), 453–475. <https://doi.org/10.1146/annurev-cellbio-100818-125300>.
- Nakao, M., Tsujikura, M., Ichiki, S., Vo, T.K., Somamoto, T., 2011. The complement system in teleost fish: progress of post-homolog-hunting researches. *Dev. Comp. Immunol.* 35 (12), 1296–1308. <https://doi.org/10.1016/j.dci.2011.03.003>.
- Nawaz, M., Li, X., Yue, X., Gouife, M., Huang, K., Chen, S., Ma, R., Jiang, J., Zhou, S., Jin, S., Wang, Y., Xie, J., 2022. Transcriptome profiling and differential expression analysis of the immune-related genes during the acute phase of infection with Photobacterium damsela subsp. damsela in silver pomfret (*Pampus argenteus*). *Fish Shellfish Immunol.* 131, 342–348. <https://doi.org/10.1016/j.fsi.2022.10.020>.
- Nombela, I., Requena-Platék, R., Morales-Lange, B., Chico, V., Puente-Marin, S., Ciordia, S., Mena, M.C., Coll, J., Perez, L., Mercado, L., Ortega-Villaizán, M.D.M., 2019. Rainbow trout red blood cells exposed to viral hemorrhagic septicemia virus up-regulate antigen-processing mechanisms and MHC I&II, CD86, and CD83 antigen-presenting cell markers. *Cells* 8 (5). <https://doi.org/10.3390/cells8050386>.
- Peach, C.J., Mignone, V.W., Arruda, M.A., Alcobia, D.C., Hill, S.J., Kilpatrick, L.E., Woolard, J., 2018. Molecular pharmacology of VEGF-A isoforms: binding and signalling at VEGFR2. *Int. J. Mol. Sci.* 19 (4). <https://doi.org/10.3390/ijms19041264>.
- Penn, J.S., Madan, A., Caldwell, R.B., Bartoli, M., Caldwell, R.W., Hartnett, M.E., 2008. Vascular endothelial growth factor in eye disease. *Prog. Retin. Eye Res.* 27 (4), 331–371. <https://doi.org/10.1016/j.preteyeres.2008.05.001>.
- Qu, A., Bai, Y., Zhang, X., Zeng, J., Pu, F., Wu, L., Xu, P., Zhou, T., 2022. Tissue-specific analysis of alternative splicing events and differential isoform expression in large

- yellow croaker (*Larimichthys crocea*) after *Cryptocaryon irritans* infection. Mar. Biotechnol. (N.Y.) 24 (3), 640–654. <https://doi.org/10.1007/s10126-022-10133-z>.
- Sangrador-Vegas, A., Martin, S.A., O'Dea, P.G., Smith, T.J., 2000. Cloning and characterization of the rainbow trout (*Oncorhynchus mykiss*) type II interleukin-1 receptor cDNA. Eur. J. Biochem. 267 (24), 7031–7037. <https://doi.org/10.1046/j.1432-1327.2000.01800.x>.
- Schmidt, C.Q., Lambris, J.D., Ricklin, D., 2016. Protection of host cells by complement regulators. Immunol. Rev. 274 (1), 152–171. <https://doi.org/10.1111/imr.12475>.
- Shen, Y., Zhang, J., Xu, X., Fu, J., Li, J., 2012. Expression of complement component C7 and involvement in innate immune responses to bacteria in grass carp. Fish Shellfish Immunol. 33 (2), 448–454. <https://doi.org/10.1016/j.fsi.2012.05.016>.
- Sokol, C.L., Luster, A.D., 2015. The chemokine system in innate immunity. Cold Spring Harb. Perspect. Biol. 7 (5) <https://doi.org/10.1101/cshperspect.a016303>.
- Stansberg, C., Subramaniam, S., Collet, B., Secombes, C.J., Cunningham, C., 2005. Cloning of the Atlantic salmon (*Salmo salar*) IL-1 receptor associated protein. Fish Shellfish Immunol. 19 (1), 53–65. <https://doi.org/10.1016/j.fsi.2004.11.006>.
- Swain, B., Basu, M., Samanta, M., 2013. NOD1 and NOD2 receptors in *mrigal* (*Cirrhinus mrigala*): inductive expression and downstream signalling in ligand stimulation and bacterial infections. J. Biosci. 38 (3), 533–548. <https://doi.org/10.1007/s12038-013-9330-y>.
- Tasdemir, E., Maiuri, M.C., Galluzzi, L., Vitale, I., Djavaheri-Mergny, M., D'Amelio, M., Criollo, A., Morselli, E., Zhu, C., Harper, F., Nannmark, U., Samara, C., Pinton, P., Vicencio, J.M., Carnuccio, R., Moll, U.M., Madeo, F., Paterlini-Brechot, P., Rizzuto, R., Szabadkai, G., Pierron, G., Blomgren, K., Tavernarakis, N., Codogno, P., Cecconi, F., Kroemer, G., 2008. Regulation of autophagy by cytoplasmic p53. Nat. Cell Biol. 10 (6), 676–687. <https://doi.org/10.1038/ncb1730>.
- Teng, J., Zhao, Y., Meng, Q.L., Zhu, S.R., Chen, H.J., Xue, L.Y., Ji, X.S., 2022. Transcriptome analysis in the spleen of northern snakehead (*Channa argus*) challenged with *Nocardia seriolae*. Genomics 114 (3), 110357. <https://doi.org/10.1016/j.ygeno.2022.110357>.
- Thaiss, C.A., Levy, M., Itav, S., Elinav, E., 2016. Integration of innate immune signaling. Trends Immunol. 37 (2), 84–101. <https://doi.org/10.1016/j.it.2015.12.003>.
- Vijay, K., 2018. Toll-like receptors in immunity and inflammatory diseases: past, present, and future. Int. Immunopharmacol. 59, 391–412. <https://doi.org/10.1016/j.intimp.2018.03.002>.
- Wang, F., Wang, X., Liu, C., Chang, O., Feng, Y., Jiang, L., Li, K., 2017. *Nocardia seriolae* infection in cultured jade perch, *Scortum barcoo*. Aquac. Int. 6, 25.
- Wang, Q., Peng, C., Yang, M., Huang, F., Duan, X., Wang, S., Cheng, H., Yang, H., Zhao, H., Qin, Q., 2021. Single-cell RNA-seq landscape midbrain cell responses to red spotted grouper nervous necrosis virus infection. PLoS Pathog. 17 (6), e1009665. <https://doi.org/10.1371/journal.ppat.1009665>.
- Wang, S., Gao, Y., Shu, C., Xu, T., 2015. Characterization and evolutionary analysis of duplicated C7 in miiuy croaker. Fish Shellfish Immunol. 45 (2), 672–679. <https://doi.org/10.1016/j.fsi.2015.05.042>.
- Wang, Y.D., Wang, Y.H., Hui, C.F., Chen, J.Y., 2016. Transcriptome analysis of the effect of vibrio alginolyticus infection on the innate immunity-related TLR5-mediated induction of cytokines in *Epinephelus lanceolatus*. Fish Shellfish Immunol. 52, 31–43. <https://doi.org/10.1016/j.fsi.2016.03.013>.
- Xiu, Y., Wang, Y., Bi, J., Liu, Y., Ning, M., Liu, H., Li, S., Gu, W., Wang, W., Meng, Q., 2016. A novel C-type lectin is involved in the innate immunity of *Macrobrachium nipponense*. Fish Shellfish Immunol. 50, 117–126. <https://doi.org/10.1016/j.fsi.2016.01.026>.
- Yasuike, M., Nishiki, I., Iwasaki, Y., Nakamura, Y., Fujiwara, A., Shimahara, Y., Kamaishi, T., Yoshida, T., Nagai, S., Kobayashi, T., Katoh, M., 2017. Analysis of the complete genome sequence of *Nocardia seriolae* UTF1, the causative agent of fish nocardiosis: the first reference genome sequence of the fish pathogenic *Nocardia* species. PLoS One 12 (3), e0173198. <https://doi.org/10.1371/journal.pone.0173198>.
- Yu, S., Shen, Z., Han, X., Chai, Y., Liu, Y., Liu, J., Lin, X., Cui, M., Zhang, F., Li, Q., Zhu, Q., 2020. Molecular characterization and complement activating functional analysis of a new collectin (TfCol-11) from *Trachidermus fasciatus*. Dev. Comp. Immunol. 102, 103486. <https://doi.org/10.1016/j.dci.2019.103486>.
- Zapata, A., Diez, B., Cejalvo, T., Gutiérrez-de Frías, C., Cortés, A., 2006. Ontogeny of the immune system of fish. Fish Shellfish Immunol. 20 (2), 126–136. <https://doi.org/10.1016/j.fsi.2004.09.005>.
- Zhu, K.C., Wu, M., Zhang, D.C., Guo, H.Y., Zhang, N., Guo, L., Liu, B.S., Jiang, S.G., 2020. Toll-like receptor 5 of Golden pompano *Trachinotus ovatus* (Linnaeus 1758): characterization, promoter activity and functional analysis. Int. J. Mol. Sci. 21 (16) <https://doi.org/10.3390/ijms21165916>.
- Zou, P.F., Chang, M.X., Xue, N.N., Liu, X.Q., Li, J.H., Fu, J.P., Chen, S.N., Nie, P., 2014. Melanoma differentiation-associated gene 5 in zebrafish provoking higher interferon-promoter activity through signalling enhancing of its shorter splicing variant. Immunology 141 (2), 192–202. <https://doi.org/10.1111/imm.12179>.
- Zou, P.F., Chang, M.X., Li, Y., Huan Zhang, S., Fu, J.P., Chen, S.N., Nie, P., 2015. Higher antiviral response of RIG-I through enhancing RIG-I/MAVS-mediated signaling by its long insertion variant in zebrafish. Fish Shellfish Immunol. 43 (1), 13–24. <https://doi.org/10.1016/j.fsi.2014.12.001>.